Myeloma cells downregulate adiponectin in bone marrow adipocytes via TNFalpha

Myeloma cells down-regulate adiponectin in bone marrow adipocytes via TNF-alpha

Emma V. Morris PhD,[1,2,3,] Karla J. Suchacki PhD,[4] Joseph Hocking MBiochem,[2,5] Rachel Cartwright MBiochem, [2,5] Aneka Sowman,[2,5] Beatriz Gamez PhD, [1,2,3,] Ryan Lea BA, [2,5] Matthew T. Drake, MD, PhD,[6] William P. Cawthorn PhD,[4] Claire M. Edwards PhD[1,2,3,5,]

[1]Nuffield Dept. of Surgical Sciences, University of Oxford, UK. [2]NIHR Oxford BRC, [3]Oxford Centre for Translational Myeloma Research, [4]University/British Heart Foundation Centre for Cardiovascular Science, The Queen's Medical Research Institute, University of Edinburgh, UK, [5]Nuffield Dept. of Orthopaedics, Rheumatology and Musculoskeletal Sciences, [6]Kogod Center on Aging and Division of Endocrinology, Mayo Clinic College of Medicine and Science, Rochester, Minnesota, USA

Grant Supporters: This work was funded by Bloodwise (C.E.), A European Union Seventh Framework Programme Marie Curie Career Integration Grant (C.E), the International Myeloma Foundation (C.E.) a Career Development Award (MR/M021394/1) from the Medical Research Council (W.P.C), a Bioinformatics Award provided through a British Heart Foundation Centre of Research Excellence grant (W.P.C), and the National Institute for Health Research (NIHR) Oxford Biomedical Research Centre (BRC). The views expressed are those of the author(s) and not necessarily those of the NHS, the NIHR or the Department of Health. Collection of samples from patients with multiple myeloma and matched controls was supported in part by the NIH/NCI (P01 CA62242).

Corresponding author:

Claire M. Edwards, Botnar Research Centre, University of Oxford, Old Road, Oxford OX3 7LD. Email: claire.edwards@ndorms.ox.ac.uk Phone; +44 (0)1865 227307

Abstract

Multiple myeloma is caused by abnormal plasma cells that accumulate in the bone marrow and interact with resident cells of the bone microenvironment to drive disease progression and development of an osteolytic bone disease. Bone marrow adipocytes (BMAds) are emerging as having important endocrine functions that can support myeloma cell growth and survival. However, how BMAds respond to infiltrating tumour cells remains poorly understood. Using the C57BL/KaLwRij murine model of myeloma, bone marrow adiposity was found to be increased in early stage myeloma with BMAds localising along the tumour-bone interface at later stages of disease. Myeloma cells were found to uptake BMAd-derived lipids *in vitro* and *in vivo* although, lipid uptake was not associated with the ability of BMAds to promote myeloma cell growth and survival. However, BMAd-derived factors were found to increase myeloma cell migration, viability and the evasion of apoptosis. BMAds are a major source of adiponectin, which is known to be myeloma-suppressive. Myeloma cells were found to down-regulate adiponectin specifically in a model of BMAds, but not in white adipocytes. The ability of myeloma cells to down-regulate adiponectin was dependent at least in part on tumour-derived TNF-alpha. Collectively our data support the link between increased bone marrow adiposity and myeloma progression. By demonstrating how myeloma cells release TNF-alpha to down-regulate BMAd-derived adiponectin, we reveal a new mechanism by which myeloma cells alter the bone microenvironment to support disease progression.

Keywords: multiple myeloma, bone marrow adipose tissue, adipocyte, adiponectin, cancer

Introduction

Multiple myeloma is an incurable haematological malignancy associated with clonal expansion of plasma cells within the bone marrow and the development of lytic bone disease. For many years it has been recognised that the success of myeloma cells to thrive within the bone marrow is in part due to their ability to interact favourably with the bone microenvironment. Myeloma cells can influence their neighbouring bone cells, resulting in bone destruction and the release of growth factors into the local environment that can be utilised by the myeloma cells for growth and survival, a process often referred to as the vicious cycle (1). However, the influence that myeloma cells have on other non-bone resident cells in the bone marrow is less clear. One of the most abundant cell types in the bone marrow is the adipocyte, these cells account for up to 70% of bone marrow volume in adult humans (2). Once thought of as inert space filling cells, adipocytes are now recognised as having specialised functions (3). These cells not only store energy in the form of triglycerides but also secrete important adipokines such as leptin and adiponectin. For many decades, bone marrow adipocytes (BMAds) were very much understudied and underappreciated. However, in recent years, this has changed, as their roles in metabolism (4) and cancer have started to emerge. BMAds have been implicated in cancers that metastasize to bone, such as prostate (5, 6) and breast cancer (7), as well as cancers that first become established in bone, such as acute myeloid leukaemia (8) and myeloma (9-13), where they appear to have a supporting role in fuelling cancer growth and progression and bone disease. However, the mechanisms driving this relationship remain unclear.

BMAds are thought to contribute to bone homeostasis via the bioactive molecules they secrete, leading to the activation of numerous signalling pathways in many different cell types by means of autocrine, paracrine and endocrine signalling (14). BMAds differ in their secretory profiles from

both white and brown adipocytes. Furthermore, they have been shown to up-regulate different genes when in close proximity to prostate cancer cells in comparison to subcutaneous adipocytes, suggesting that they have bone specific effects (5). Adiponectin is the most prevalent adipokine secreted by adipocytes. While adiponectin is secreted by all adipose cells, it is most highly secreted by BMAds (4, 15). Adiponectin is known to play an important role in insulin sensitivity and fatty acid oxidation and has been shown to have anti-tumour effects (16-18). Adiponectin is paradoxically decreased during conditions of elevated adiposity, and our previous studies have implicated both obesity and hypoadiponectinaemia in the progression of multiple myeloma and its associated bone disease (19-21). In the present study, we have investigated how myeloma cells alter BMAd biology in order to circumvent the tumour-suppressive effect of adiponectin.

Materials and Methods

Animal model

Animal experiments were undertaken under UK Home Office Project License 30/2996. Animals were housed in individually ventilated cages in the Department of Biomedical Services, University of Oxford, with access to normal chow and water *ad libitum*. Studies were conducted using age-, sex-, and weight-matched KaLwRij mice (Harlan Netherlands). Due to the nature of the model the speed of tumour development can vary between individual experiments. As such, 'low' and 'high' tumour burden, indicating less than an average of 10% myeloma cells in bone marrow or greater than an average of 30% myeloma cells in bone marrow respectively, was used to describe the experimental conditions, rather than days after inoculation. Mice were inoculated with 10^6 5TGM1-GFP cells or PBS vehicle control by intravenous injection. Mice were sacrificed on day 16 to represent 'low' tumour burden and day 23 to represent 'high' tumour burden post inoculation (5 controls, 7-low and 6-high tumour burden mice were used, all animals were 12 weeks of age). Investigators were not blinded throughout the experiment. In separate experiments, animals used for osmium tetroxide analysis were inoculated as above and culled on day 24 when tumour burden was less than 10%, representing a 'low' tumour burden model (4 controls and 5 inoculated, all animals were 8 weeks of age). Investigators were blinded at endpoint. Animals used for bone marrow plug analysis were inoculated as above and culled on day 23 (3 inoculated, animals were 6 months of age to ensure adequate visualisation of BMAds, all mice had detectable myeloma). To investigate the effect of the JJN-3 human cell-line *in vivo* age-, sex-, weight-matched Nod/Scid γ (NSG, NOD.Cg-Prkdcscid Il2rgtm1Wjl/SzJ) mice were purchased from Charles River. Mice were inoculated with 10^6 JJN-3 cells or PBS vehicle control by intravenous injection. Animal were

sacrificed on day 23. (5 controls and 7 inoculated, all animals were 8 weeks of age). Investigators were not blinded throughout the experiment.

Immunofluorescence

Sections from paraffin-wax-embedded tissue samples were de-waxed, and antigen retrieval was performed using citric acid buffer. Sections were incubated with 1:200 chicken anti-GFP (Invitrogen A10262) and 1:100 rabbit anti-perilipin (Cell Signaling 3470S) in 1% BSA/5% serum/phosphate buffered saline (PBS) overnight at 4°C. Sections were subsequently incubated for 1 hr at room temperature with 1:200 Alexa Fluor 488 anti-chicken (Invitrogen A11039) and Alexa Fluor 568 anti-rabbit secondary antibodies (Invitrogen A11011), and 1:5000 DAPI. Lipid uptake studies using patient samples were performed by layering the bone marrow sample over histopaque and centrifuging at 400 x g for 30 minutes. The fatty top layer of the sample was then removed and diluted 1:2 with normal media, myeloma cells were then added for 24 hrs before staining. The lipid uptake studies using cell lines were performed by liberating the lipids from ST2-derived BMAds and incubating them with myeloma cells for 24 hrs. Cells were then stained with 1:1000 BODIPY (ThermoFisher Scientific D3922) or 1:500 Lipidtox (ThermoFisher Scientific H24476) and 1:2000 Hoechst (Sigma B2261) and visualised by confocal microscopy.

Bone marrow plugs

Marrow plugs were prepared using femurs taken from 6 month old mice that had been inoculated with 5TGM1-GFP cells for 23 days. Marrow plugs were extracted and fixed on slides (22). The samples were then washed with PBS and stained using 1:500 Lipidtox (ThermoFisher Scientific H24476) for 30 minutes.

Quantification of tissue sections

Long bones were formalin-fixed, decalcified in 14% EDTA, paraffin-embedded, and sectioned along the mid-sagittal plane in 4-μm-thick sections prior to staining with haematoxylin and eosin. Histomorphometric analysis was performed to quantify BMAd number and tumour burden using Osteomeasure histomorphometry software as previously described (23) or ImageJ software.

Osmium tetroxide staining

Formalin fixed, decalcified tibiae were washed in Sorensen's Phosphate buffer (81 mM KH2PO4, 19 mM Na2HPO4 · 7H2O, pH 7.4) and stained with 1% osmium tetroxide solution (2% w/v; Agar Scientific, UK - diluted 1:1 in Sorensen's Phosphate buffer) for 48 hrs at room temperature, washed, and stored in Sorensen's Phosphate buffer at 4 °C. Stained tibiae were arranged in parallel in 1% agarose in a 30-mL universal tube and mounted in a Skyscan 1172 desktop micro CT (Bruker, Kontich, Belgium). The samples were then scanned through 360° using a step of 0.40° between exposures. A voxel resolution of 12.05 μm was obtained in the scans using the following control settings: 54 kV source voltage, 185 μA source current with an exposure time of 885 ms. A 0.5-mm aluminium filter and two-frame averaging were used to optimize the scan. After scanning, the data were reconstructed using Skyscan software NRecon v1.6.9.4 (Bruker, Kontich, Belgium). The reconstruction thresholding window was optimised to encapsulate the target image. Volumetric analysis was performed using CT Analyser v1.13.5.1 (Bruker, Kontich, Belgium) (24).

Cell culture and adipocyte differentiation

The 5TGM1-GFP and JJN-3 myeloma cell lines were cultured in RPMI media supplemented with 10% fetal bovine serum (FBS), 2 mM L-glutamine, 1 mM Sodium Pyruvate, 0.1 mM Non-Essential Amino Acids, and 100 U/ml Penicillin-Streptomycin antibiotic, and incubated at 37°C with 5% CO_2. ST2 cells were seeded in RPMI media (supplemented as above) in 6-well plates at a density of $8x10^5$ per well. After 24 hrs the media was changed to adipogenic media containing

0.5 mM IBMX, 0.25 µM dexamethasone and 10 µg/ml insulin. Cells were then incubated for 3 days, after which the media was changed to maintenance media containing insulin alone, and cells were then incubated for a further 3 days. Media was then changed to normal RPMI media and incubated for 24 hrs before the cells were used. Human bone marrow stromal cells (BMSCs) were grown in DMEM containing 20% FBS. Upon reaching 70% confluency, culture media was changed for adipogenic media (DMEM + 10%FBS) containing 0.5 mM IBMX, 1 µM dexamethasone, 100 nM insulin and 0.2 mM indomethacin. Media was replenished every 3 days for 21 days. Media was then changed to RPMI and cells were incubated for 24 hrs before use. Cell differentiation was confirmed using Oil red O staining according to the manufacturer's instructions. Co-culture experiments were carried out using transwell inserts (Scientific Laboratory Supplies 353090) which were added to the plates after the differentiation process. Myeloma cells were then plated in the inserts at a density of $1.5x10^6$ and left for 24, 48 or 72 hrs.

Lipid Uptake Studies

Myeloma cells were treated with limiting growth media (RPMI with no glucose or supplements) for 24 hrs. Cells were then treated with a 1:1 mix of limiting growth media, limiting growth media and normal media, limiting growth media and BMAd-derived lipid or limiting growth media and BMAd 24 hr conditioned media, for a further 24 hrs. BMAd-derived lipid was liberated by scraping the BMAd cells and then centrifuging them at 17,000g for 5 minutes. The white lipid layer was then removed from the top of the media. 150 µl of lipid was added to 600 ul of limiting growth media to make up the BMAd lipid mixture. BMAd conditioned media was media incubated with BMAds for 24 hrs. Cells were then seeded in a 96-well plate for Alamar Blue analysis or in confocal dishes for visualisation.

Oil Red O Quantification

Oil red O stain was eluted using 1ml of isopropanol for 10 minutes. The absorbance of the elution was measured at a wavelength of 518nm. Eluted stain from undifferentiated ST2 cells was used as a blank.

Viability assay

Myeloma cells were seeded in normal RPMI media as described previously at a density of $7.5x10^5$/ml in transwell inserts alone or in co-culture with undifferentiated BMSCs or BM-like adipocytes derived from ST2 cells. Cells were re-plated in a 96 well plate at each time point. 10% Alamar Blue was added and cells were incubated for 3 hrs. Fluorescence intensity was measured using a FLUOstar omega plate reader.

Migration assay

Boyden chambers (Costar 3422) were used according to the manufacturer's instructions. The lower chambers contained either 800 µL normal media, 50% conditioned media taken from undifferentiated ST2 BMSCs (control), or 50% conditioned media from adipocytes derived from ST2 cells. Cells were seeded in the top chamber at a density of $4x10^5$ in 200 uL of 1% FBS media. After 24 hrs viability of the cells in the lower chamber was measured using Alamar Blue.

Patient samples

Serum samples from patients with multiple myeloma, and the respective age- and sex-matched controls (n=20, 15M, 5F, age 62.95 years ± 10.7), were obtained through collaboration with MTD and with approval from the Institutional Review Board and Biospecimen Protocol Review Group of the Mayo Clinic College of Medicine. All patients were newly diagnosed myeloma patients (M-Spike 2.61g/dL ± 1.99 g/dL, 12/15 patients had evidence of bone disease as indicated by osteoporosis and or lytic lesions or fracture. Bone marrow samples from patients with, or under

investigation for, myeloma were obtained with the approval of the Oxford Clinical Research Ethics Committee (09/H0606/5+5 project 16/A185).

QPCR

RNA from cell lines and primary BMSCs was isolated using the RNeasy kit (QIAGEN). cDNA was generated using Precision Reverse Transcription Premix kit (Primerdesign). Mouse adiponectin was detected by real-time PCR using Sybr green primers (Life Tech). Relative gene expression of adiponectin was normalized to gene expression for *Gapdh* (Life Tech). Primer sequences: mAdiponectin F: AGACCTGGCCACTTTCTCCTCATT; mAdiponectin R: AGAGGAACAGGAGAGCTTGCAAGA; mGAPDH F: TCAACAGCAACTCCCACTCTTC CA; mGAPDH R: ACCCTGTTGCTGTAGCCGTATTCA. QuantiTech Primers for Adipsin, Visfatin and Resistin were purchased from Qiagen and used according to the manufacturer's instructions.

Immunoblotting and ELISA

Immunoblotting was used to measure apoptosis and adiponectin expression following a standard Bio-Rad protocol. The primary antibodies used were 1:1000 rabbit anti-cleaved PARP (Cell Signaling 5625), 1:1000 rabbit anti-cleaved caspase-3 (Cell Signaling 9664), 1:1000 rabbit anti-adiponectin (Abcam ab3455) 1:1000 rabbit anti-phospho-c-Jun N-terminal kinases (p-JNK; Thr183/Tyr185) (Cell signaling 9251), 1:1000 rabbit anti-total JNK (T-JNK) (Cell signaling 9252), 1:1000 rabbit anti-phospho-p38 mitogen-activated protein kinases (p-p38 MAPK; Thr180/Tyr182) (Cell signaling 4092), 1:1000 rabbit anti-total p38 MAPK (T-p38 MAPK) (Cell signaling 8690), 1:1000 rabbit anti-phospho-p44/42 MAPK [phospho-extracellular signal-related kinases 1 and 2 (p-ERK1/2); Thr202/Tyr204] (Cell signaling 9101), 1:1000 rabbit anti-total p44/42 MAPK (T-ERK1/2) (Cell signaling 9102), and 1:10,000 mouse anti-β actin (Sigma A5316). All

secondary antibodies were purchased from Cell Signaling. An ELISA was used to measure adiponectin (R&D systems MRP300) and TNF-α (R&D systems MHSTA50) according to the manufacturer's instructions.

mRNA Stability Assay

ST2 derived BMAds were treated with recombinant TNF-α for 24 h, 10μg/ml of Actinomycin D was then added, cells were collected at 0, 1, 2, 4 and 6 h following treatment. Levels of adiponectin gene expression was measured using qPCR.

TNF-α neutralisation

Cytokine blocking was achieved using an antibody directed against mouse TNF-α (R&D Systems MAB4101). Co-cultures of myeloma cells and mature adipocytes were treated with anti-TNF-α at a concentration of 1.5 μg/ml, or isotype control. Treated cells were left for 24 hrs (5TGM1) or 48 hrs (JJN-3) before conditioned media and RNA were collected.

Statistical Analyses

Statistical significance was determined using a Mann-Whitney U Test, Unpaired t-test, Pearson correlation or one-way ANOVA and TUKEY-Kramer posthoc test. Significance was considered for $p<0.05$. Datasets from *in vivo* analysis were based on groups of animals. *In vitro* experiments were performed a minimum of three separate occasions. Data are represented as mean ± SE unless otherwise stated.

Results

Bone marrow adiposity is increased in early stage myeloma.

To investigate the effect of myeloma cells on BMAd localisation and number, the well-established Radl model of myeloma was used (25, 26). This model successfully recapitulates human disease with 5TGM1 cells homing to bone where they become established and cause bone lesions (27, 28). First we analysed KaLwRij mice with low tumour burden using osmium tetroxide staining of their tibiae (Figure 1A). These mice had significantly higher bone adiposity compared to controls (Figure 1B), and this increase in adiposity was primarily confined to the distal tibia, suggesting that the increase is within the constitutive BMAd population (29). We did not observe any changes in the adipocytes that reside in the proximal tibia, although this may reflect the sensitivity of osmium-tetroxide based detection. To investigate this further, mice were culled 16- and 23-days post inoculation to mimic low and high tumour burden, reflecting early and late-stage disease. Immunofluorescence of the femurs confirmed the presence of GFP-positive tumour cells (denoted by white line), as well as identifying BMAds morphologically using adipocyte marker, perilipin (Figure 1C, Supplemental Figure 1). We observed that the BMAds present in the 23-day mice were predominantly located along the tumour-bone interface (Figure 1C, red dotted line), with a change in the ratio of BMAds outside the tumour area:within the tumour area from 9:1 in the low tumour burden mice to 1:1 in the high tumour burden mice (Figure 1D). Similar localisation of BMAds along the tumour-bone interface was observed in a JJN-3 model of myeloma (Supplemental Figure 2). Paraprotein levels and tumour burden were significantly higher in the mice with high tumour burden compared to low (Figure 1E and F), indicating significant disease progression from less than 10% plasma cells within the bone marrow to greater than 30% marrow infiltration. The number of BMAds present in low tumour mice was significantly higher in plasma-cell inoculated

mice than compared to control. However, this increase was not observed in the high tumour mice (Figure 1G).

BMAds support myeloma growth by a lipid-independent mechanism

Our discovery that myeloma cells promote an increase in the number of BMAds at early stages of disease *in vivo*, combined with previous studies suggesting that BMAds are supportive of myeloma growth (9, 30), led us to consider how BMAds can confer a survival advantage to myeloma cells. Our studies confirm the myeloma-supportive effects of BMAds, with a significant increase in myeloma cell viability and decrease in apoptosis when myeloma cells were cultured with either BMAds or BMSCs, and an increase in migration towards media conditioned from BMAds (Figure 2A - D).

BMAds are a major source of lipid, and prostate cancer cells are known to uptake adipocyte derived lipids to promote cell viability (5). This led us to investigate whether myeloma cells behave in a similar manner. Visualisation of lipid droplets demonstrated that JJN-3 myeloma cells were able to uptake lipids isolated from the bone marrow of patients with myeloma (Figure 3A). However, when JJN-3 or 5TGM1 myeloma cells were incubated with liberated lipid droplets from BMSCs or BMAds, the amount of lipid uptake was significantly different between the myeloma cells, with limited lipid uptake detected in 5TGM1 myeloma cells (Figure 3B, C and D). Next, we investigated whether lipid uptake had a positive effect on myeloma cell viability. There was no difference in viability between JJN-3 or 5TGM1 myeloma cells that had been incubated with or without BMAd-derived lipid (Figure 3E). Cells were then placed under metabolic stress to establish whether by inducing a stress response, they may utilise lipid for survival. Myeloma cells were grown in limiting condition media (RPMI with no glucose, supplements or FBS) for 24 hrs and then incubated with liberated lipid or conditioned media from BMAds. Interestingly, the

culture of myeloma cells in limiting conditions resulted in the appearance of lipidtox-positive cells, indicative of de novo lipogenesis (Figure 4A). A trend towards increased viability was observed when myeloma cells were cultured in limiting conditions and then exposed to BMAd-derived lipid. However, conditioned media taken from BMAds was found to significantly increase viability compared to both the control and the BMAd-derived lipid (Figure 4B). To determine whether lipid is present within myeloma cells *in vivo,* we used a technique to visualise the bone marrow by extracting fresh marrow with a needle and fixing and staining it immediately (22). Using this technique, we were only able to detect the presence of lipid in a very small number of 5TGM1-GFP cells present in the bone marrow *in vivo* (Figure 4C and Supplemental figure 3). Furthermore, it is not possible to conclude whether these lipid droplets were from neighbouring BMAds or a product of de novo lipogenesis.

Myeloma cells down-regulate adiponectin in BMAds

Our studies reveal a myeloma-promoting effect of BMAds that does not appear to be related to lipid uptake. To reconcile our findings that BMAds are increased and protect myeloma cells despite the known tumour-suppressive effects of adiponectin (16), we investigated whether myeloma cells down-regulate adiponectin in BMAds. Quantitation of circulating adiponectin revealed a significant reduction in adiponectin in patients with multiple myeloma, and in myeloma-bearing mice (Figure 5A and B). Co-cultures of myeloma cells with BMSCs or BMAds demonstrated that adiponectin was significantly down-regulated in the ST2-derived BMAds that had been co-cultured with myeloma cells as compared to BMAds cultured with media alone. This was observed in both cell lysates and CM at the protein level (Figure 5C and D) as well as at the RNA level (Figure 5E). To further confirm the down-regulation of adiponectin in BMAds, primary myeloma cells were co-cultured with ST2-derived BMAds (Figure 5F), again showing a decrease

in adiponectin levels following 24 hrs of co-culture. This reduction was not observed after 72 hrs in the cell lysates, however, this may be a reflection of low primary cell viability after 72 hrs of culture. Similar experiments were performed using 3T3-L1 adipocytes. Adiponectin secretion was lower in 3T3-L1 adipocytes than in ST2-derived BMAds, confirming that the former are more WAT-like. (Supplemental Figure 4A), However, unlike in ST2-derived BMAds, myeloma cells did not further decrease adiponectin expression in 3T3-L1 adipocytes, suggesting that the ability of myeloma cells to down-regulate adiponectin is specific to BMAds (Supplemental Figure 4B).

Myeloma cells down-regulate adiponectin in BMAds via TNF-a

Our data demonstrates that myeloma cells down-regulate adiponectin in BMAds. However, the mechanism behind this down-regulation remains unknown. Co-culture of myeloma cells with BMAds, either in direct contact or separated by a transwell membrane, was found to have a modest effect to reduce BMAd number and size (Figure 6A-F). Investigation of additional adipokines did not reveal a generalised loss in adipokine secretion, with no significant difference in expression of resistin, visfatin or adipsin (Figure 6G). This suggests a specific mechanism underlying the down-regulation of adiponectin in BMAds by myeloma cells. Myeloma cells secrete a number of cytokines known to drive disease progression, one of which is TNF-alpha (31, 32). Measurement of TNF-α in the bone marrow plasma of myeloma-bearing mice demonstrated a significant correlation with tumour burden, confirming an association with disease progression (Figure 7A). Previously TNF-α has been implicated as a potential regulator of adiponectin expression in WAT, but not in the context of cancer (33-35). Transwell co-culture of myeloma cells with BMAds was found to increase activation of JNK, p38MAPK and ERK1/2, pathways which have previously been implicated in TNF-α-mediated suppression of adiponectin in WAT (36) (Figure 7B). TNF-α treatment alone did not induce theses changes in BMAds suggesting that WAT may be more

sensitive to TNF-α alone. To determine whether TNF-α could regulate adiponectin in BMAds, we treated ST2-derived bone marrow BMAds with mouse recombinant TNF-α. After 24 hrs and 48 hrs, there was a 65% and 50% respective decrease in *Adipoq* expression (Figure 7C) and in secreted adiponectin (Figure 7D). A smaller reduction in *Adipoq* expression (41%) was observed after 72 hrs suggesting a level of recovery from the initial TNF-α exposure. TNF-α treatment also resulted in a significant difference in *Adipoq* mRNA stability following 2hrs treatment with the transcriptional inhibitor actinomycin D, but no overall change in mRNA half-life (Supplemental Figure 5). The addition of recombinant TNF-α to mature BMAds cultures for 72 hrs also caused a reduction in Oil Red O staining indicating a decreased in BMAd number in a similar manner to myeloma/BMAd co-culture (Figure 7E). To determine whether the down-regulation of adiponectin was due to myeloma-derived TNF-α, a TNF-α blocking antibody was used. Adiponectin secretion (Figure 7F-G) and *Adipoq* expression (Figure 7H and Supplemental Figure 6A) were decreased in co-cultures containing either 5TGM1 or JJN-3 myeloma cells alone or in the presence of an isotype control antibody. In contrast, addition of a neutralizing antibody to TNF-α to myeloma/BMAd co-cultures had no effect on viability (Supplemental Figure 6B) but blocked the suppression of adiponectin and prevented the reduction in BMAd number (Figure 7I and Supplemental Figure 6C).

Discussion

There is growing evidence that BMAds play an important role in a number of different cancers that metastasise to (breast and prostate), or develop within the bone such as myeloma. Our study advances these previous findings by providing a mechanism by which myeloma cells interact with BMAds to circumvent the tumour-suppressive effect of adiponectin.

Using our murine myeloma model, we have shown that in early stage disease (defined clinically as less than 10% myeloma cells present within the bone marrow) there is a significant increase in marrow adiposity. This is supported by previous studies that revealed that bone marrow from patients with myeloma contained increased pre-adipocytes and significantly larger mature adipocytes than bone marrow obtained from healthy volunteers, and that adipogenic gene expression is elevated in mesenchymal stem cells from myeloma-bearing mice (10, 12). Our data shows an increase in overall adiposity volume, which could be due to either increased BMAd size, number, or both. This increase may be in response to the initial influx of cancer cells, as it is not observed in late disease. Although, this finding is to be expected, as in end-stage disease the myeloma cells have substantially increased in number and both modulate bone cell numbers and behaviour, and also physically crowd out other cells within the bone marrow microenvironment. Therefore, the observed change in ratio from BMAds localised outside the tumour area to BMAds inside the tumour area in the high tumour-bearing mice may be a simple reflection of increased tumour burden. However, interestingly the remaining BMAds were shown to be lining the tumour-bone interface suggesting that BMAd localisation is affected by the infiltrating tumour cells. Whether these BMAds are recruited by the tumour cells, whether BMAds within the tumour area are destroyed by the infiltrating tumour cells leaving only the cells surrounding the tumour, or whether the remaining BMAds shrink in size but persist in the marrow, remains unclear. Our *in*

vitro studies demonstrate a small reduction in BMAd number and size following culture with myeloma cells, supporting our *in vivo* findings in late-stage myeloma. The initial increase in adiposity that we observed suggests that BMAds have a positive impact on disease progression. An intriguing finding was that the increase in adiposity appeared most prominently in the distal section of bone. BMAds are proposed to exist in two broad sub-types; regulated and constitutive. Regulated BMAds are found in the more metabolically active regions of the bone and are thought to be responsible for responding to environmental cues such as changes in diet or exercise. Constitutive BMAds develop early in life and are rarely depleted, and are thought to be less responsive than regulated (3). However, in our study, we identified an increase in marrow adiposity in the distal tibia, the site at which constitutive BMAds reside. One possibility is that myeloma does impact the regulated BMAds but that, in our model these cells remain too diffuse to be detectable by osmium tetroxide staining. Indeed, KaLwRij mice are a sister strain of the B6 mouse which have low levels of regulated fat until later in life (29). At younger ages, as in our mice, regulated BMAds are dispersed among hematopoietic cells, whereas constitutive BMAds are clustered together resembling the tightly packed structure of adipocytes in WAT. As such, our findings in the distal tibia might reflect, the sensitivity of the osmium staining for detection of clusters of BMAds as opposed to single cells. If so, in our model, changes in regulated BMAds within the metaphyseal region may be below the level of detection using this approach. It is also possible that early changes occur in regulated BMAds residing close to the constitutive region, but that these changes are too subtle to detect. Alternatively, it may be that myeloma cells modify only the constitutive BMAds. It must also be acknowledged that a limitation of the study is that histological analysis was performed on femurs and osmium tetraoxide on tibiae, and it is of interest

to determine whether changes in constitutive BMAds are also observed in femoral bone. Formally addressing these questions in future studies is warranted.

Our findings also provide evidence to support the growing belief that BMAd interactions are advantageous for myeloma cell viability and evasion of apoptosis, and that adipogenic factors promote myeloma cell migration (9-11). Interestingly, we also observed that BMSCs offer a significant level of support in promoting viability and evading apoptosis, this raises the question as to the similarities between these two cell types and the factors they secrete. In contrast, BMAds significantly increased the migration rates of myeloma cells compared to BMSCs. This is in line with other studies in different tumour types that have a propensity to metastasise to bone, one study showed that breast cancer cells have increased migration towards human bone tissue-conditioned medium (7), and another that prostate cancer cells interact with BMAds resulting in the promotion of growth and invasiveness driven by BMAd-derived lipids from nearby BMAds (5). These observations raise the questions as to whether myeloma cells are attracted to factors secreted by BMAds, or whether myeloma cells need to utilise the BMAd's lipid storage in a manner similar to prostate tumour cells or whether both elements are important. We have shown that conditioned media rich in BMAd-derived factors promotes myeloma cell growth and migration. Furthermore, we have also shown that myeloma cells are capable of BMAd-derived lipid uptake *in vitro*, however, striking differences were found between myeloma cell lines. Interestingly we did not observe a difference in viability when liberated BMAd-derived lipid was added to normal culture media. However, we did observe a trend towards elevated viability when myeloma cells were cultured in growth-limiting conditions, and then liberated lipid was added, suggesting that lipids may be utilised in times of stress. In addition, growth-limiting conditions alone induced de novo lipogenesis in myeloma cells, suggesting a selective dependence upon exogenous lipid as an

energy source that warrants further investigation. In vivo, the presence of lipid was detectable in a small proportion of myeloma cells in the bone marrow of myeloma-bearing mice. While it is not possible to distinguish between lipid uptake and de novo lipogenesis *in vivo*, the small proportion of myeloma cells with detectable lipid may suggest a limited role for lipid in myeloma growth in the bone marrow. Notably, while there is a marked difference in lipid uptake between 5TGM1 and JJN-3 myeloma cells *in vitro*, the *in vivo* preclinical models are strikingly similar with respect to tumour burden and osteolytic bone disease. Furthermore, we show that localisation of BMAds along the tumour-bone interface is comparable between models. Taken together, our data suggests a limited role for lipid uptake in disease pathogenesis. Future studies are needed to elucidate whether lipids supply valuable energy for cell motility and/or invasiveness, or whether they may play a direct role in conferring a level of drug resistance.

Most research in the adipocyte-cancer field implicates the adipocyte as a cell that promotes tumour growth. However, adipocytes do not only secrete tumour-promoting factors. One adipokine known to have potent anti-tumour effects is adiponectin, the most highly expressed adipokine in the WAT. However, low adiponectin levels are associated with a variety of disorders including coronary heart disease (37), type 2 diabetes (38, 39), obesity and cancer (40). Interestingly, a number of these conditions have also been associated with high levels of TNF-α (41-43). Patients with myeloma were shown to have significantly higher levels of TNF-α compared to healthy volunteers, with levels rising in association with disease progression. (44). Our murine data supports these findings, showing that levels of TNF-α also correlate with tumour burden and that mice inoculated with myeloma cells also have significantly lower adiponectin levels. These findings extend our previous studies, where we found that adiponectin was reduced in myeloma-permissive mice (16). However, the mechanism(s) that links these two proteins in the development of myeloma is

unknown. TNF-α is known to regulate adiponectin production in WAT. We now show that TNF-α is able to downregulate adiponectin in ST2-derived BMAds, likely dependent on both transcriptional regulation and loss of mRNA stability. More importantly we show that myeloma cells are able to manipulate their environment by down-regulating adiponectin in these BMAds, at least in part via the secretion of TNF-α. Interestingly, viability was not altered by blockade of TNF-alpha, suggesting additional mechanisms may contribute to the effect of BMAds on myeloma cell viability. Moreover, the addition of recombinant TNF-α also caused a change in BMAd number in a similar manner to myeloma /BMAds co-cultures. This reduction in adiposity may also contribute to lower levels of adiponectin, especially in late stage disease as the myeloma cells start to over populate the marrow and directly interact with the majority of remaining BMAds. The addition of a TNF-α neutralising antibody restored both adiponectin expression levels and BMAd number, however, interestingly, viability was not altered by blockade of TNF-α, suggesting additional mechanisms may contribute to the effect of BMAds on myeloma cell viability. Elevated levels of TNF-α have long been associated with myeloma, and our results provide new insights into the mechanisms by which this key inflammatory cytokine promotes myeloma disease progression.

Collectively, our studies provide new insights into the BMAd-myeloma cell interaction *in vivo*, revealing a new mechanism by which myeloma cells alter their microenvironment to support their growth. BMAd-derived factors are utilised for growth and survival and in order to fully take advantage of this relationship, myeloma cells have developed a valuable mechanism to down-regulate adiponectin to thereby evade its anti-tumour effects. Future studies are needed to further investigate and understand the contribution of BMAd-derived lipids and whether they play a significant role in myeloma disease progression. Once thought of as an inert space filling cell,

BMAds are slowly emerging as fundamental to disease progression. As society battles against the burgeoning obesity epidemic, efforts to more fully understand the implications of increased bone marrow adiposity for tumour growth and survival within bone will become increasingly important.

ACKNOWLEDGEMENTS

We thank the patients who donated clinical samples used in this research. This work was funded by Bloodwise (C.E.), A European Union Seventh Framework Programme Marie Curie Career Integration Grant (C.E), a Career Development Award (MR/M021394/1) from the Medical Research Council (W.P.C), a Bioinformatics Award provided through a British Heart Foundation Centre of Research Excellence grant (W.P.C), and the National Institute for Health Research (NIHR) Oxford Biomedical Research Centre (BRC). The views expressed are those of the author(s) and not necessarily those of the NHS, the NIHR or the Department of Health. Collection of samples from patients with multiple myeloma and matched controls was supported in part by the NIH/NCI (P01 CA62242). The authors have no conflicts of interest to declare.

AUTHORS' ROLES

EVM devised and performed experiments, analysed data and prepared manuscript. KS, JH, RC, BG, RL performed experiments and analysed data. MTD provided patient serum samples and discussed analyses. WC contributed conceptually and discussed analyses. CME supervised research, devised experiments, reviewed data and prepared manuscript. All authors have read and reviewed the manuscript.

References

1. Mundy GR. Mechanisms of bone metastasis. Cancer. 1997;80(8 Suppl):1546-56.

2. Fazeli PK, Horowitz MC, MacDougald OA, Scheller EL, Rodeheffer MS, Rosen CJ, et al. Marrow fat and bone--new perspectives. J Clin Endocrinol Metab. 2013;98(3):935-45.

3. Scheller EL, Rosen CJ. What's the matter with MAT? Marrow adipose tissue, metabolism, and skeletal health. Annals of the New York Academy of Sciences. 2014;1311:14-30.

4. Cawthorn WP, Scheller EL, Learman BS, Parlee SD, Simon BR, Mori H, et al. Bone marrow adipose tissue is an endocrine organ that contributes to increased circulating adiponectin during caloric restriction. Cell Metab. 2014;20(2):368-75.

5. Herroon MK, Rajagurubandara E, Hardaway AL, Powell K, Turchick A, Feldmann D, et al. Bone marrow adipocytes promote tumor growth in bone via FABP4-dependent mechanisms. Oncotarget. 2013;4(11):2108-23.

6. Hardaway AL, Herroon MK, Rajagurubandara E, Podgorski I. Marrow adipocyte-derived CXCL1 and CXCL2 contribute to osteolysis in metastatic prostate cancer. Clin Exp Metastasis. 2015;32(4):353-68.

7. Templeton ZS, Lie WR, Wang W, Rosenberg-Hasson Y, Alluri RV, Tamaresis JS, et al. Breast Cancer Cell Colonization of the Human Bone Marrow Adipose Tissue Niche. Neoplasia. 2015;17(12):849-61.

8. Shafat MS, Oellerich T, Mohr S, Robinson SD, Edwards DR, Marlein CR, et al. Leukemic blasts program bone marrow adipocytes to generate a protumoral microenvironment. Blood. 2017;129(10):1320-32.

9. Liu Z, Xu J, He J, Liu H, Lin P, Wan X, et al. Mature adipocytes in bone marrow protect myeloma cells against chemotherapy through autophagy activation. (1949-2553 (Electronic)).

10. Trotter TN, Gibson JT, Sherpa TL, Gowda PS, Peker D, Yang Y. Adipocyte-Lineage Cells Support Growth and Dissemination of Multiple Myeloma in Bone. (1525-2191 (Electronic)).

11. Caers J, Deleu S, Belaid Z, De Raeve H, Van Valckenborgh E, De Bruyne E, et al. Neighboring adipocytes participate in the bone marrow microenvironment of multiple myeloma cells. Leukemia. 2007;21(7):1580-4.

12. Berlier JL, Rethnam M, Banu Binte Abdul Majeed A, Suda T. Modification of the bone marrow MSC population in a xenograft model of early multiple myeloma. Biochem Biophys Res Commun. 2019;508(4):1175-81.

13. Liu H, He J, Koh SP, Zhong Y, Liu Z, Wang Z, et al. Reprogrammed marrow adipocytes contribute to myeloma-induced bone disease. Sci Transl Med. 2019;11(494).

14. Rosen CJ, Ackert-Bicknell C, Rodriguez JP, Pino AM. Marrow Fat and the Bone Microenvironment: Developmental, Functional, and Pathological Implications. Critical reviews in eukaryotic gene expression. 2009;19(2):109-24.

15. Swarbrick MM, Havel PJ. Physiological, pharmacological, and nutritional regulation of circulating adiponectin concentrations in humans. Metabolic syndrome and related disorders. 2008;6(2):87-102.

16. Fowler JA, Lwin ST, Drake MT, Edwards JR, Kyle RA, Mundy GR, et al. Host-derived adiponectin is tumor-suppressive and a novel therapeutic target for multiple myeloma and the associated bone disease. Blood. 2011;118(22):5872-82.

17. Saxena NK, Sharma D. Metastasis suppression by adiponectin: LKB1 rises up to the challenge. Cell adhesion & migration. 2010;4(3):358-62.

18. Man K, Ng KTP, Xu A, Cheng Q, Lo CM, Xiao JW, et al. Suppression of Liver Tumor Growth and Metastasis by Adiponectin in Nude Mice through Inhibition of Tumor Angiogenesis

and Downregulation of Rho Kinase/IFN-Inducible Protein 10/Matrix Metalloproteinase 9 Signaling. Clinical Cancer Research. 2010.

19. Hofmann JN, Birmann BM, Teras LR, Pfeiffer RM, Wang Y, Albanes D, et al. Low Levels of Circulating Adiponectin Are Associated with Multiple Myeloma Risk in Overweight and Obese Individuals. Cancer Res. 2016;76(7):1935-41.

20. Dalamaga M, Christodoulatos GS. Adiponectin as a biomarker linking obesity and adiposopathy to hematologic malignancies. Hormone molecular biology and clinical investigation. 2015;23(1):5-20.

21. Dalamaga M, Karmaniolas K Fau - Panagiotou A, Panagiotou A Fau - Hsi A, Hsi A Fau - Chamberland J, Chamberland J Fau - Dimas C, Dimas C Fau - Lekka A, et al. Low circulating adiponectin and resistin, but not leptin, levels are associated with multiple myeloma risk: a case-control study. (1573-7225 (Electronic)).

22. Horowitz MC, Berry R, Holtrup B, Sebo Z, Nelson T, Fretz JA, et al. Bone marrow adipocytes. Adipocyte. 2017;6(3):193-204.

23. Edwards CM, Edwards JR, Lwin ST, Esparza J, Oyajobi BO, McCluskey B, et al. Increasing Wnt signaling in the bone marrow microenvironment inhibits the development of myeloma bone disease and reduces tumor burden in bone in vivo. Blood. 2008;111(5):2833-42.

24. McIlroy GD, Suchacki K, Roelofs AJ, Yang W, Fu Y, Bai B, et al. Adipose specific disruption of seipin causes early-onset generalised lipodystrophy and altered fuel utilisation without severe metabolic disease. Molecular metabolism. 2018;10:55-65.

25. Radl J, Croese JW, Zurcher C, Van den Enden-Vieveen MH, de Leeuw AM. Animal model of human disease. Multiple myeloma. The American journal of pathology. 1988;132(3):593-7.

26. Radl J, De Glopper E, Schuit HRE, Zurcher C. Idiopathic Paraproteinemia. The Journal of Immunology. 1979;122(2):609.

27. Garrett IR, Dallas S, Radl J, Mundy GR. A murine model of human myeloma bone disease. Bone. 1997;20(6):515-20.

28. Dallas SL, Garrett IR, Oyajobi BO, Dallas MR, Boyce BF, Bauss F, et al. Ibandronate Reduces Osteolytic Lesions but not Tumor Burden in a Murine Model of Myeloma Bone Disease. Blood. 1999;93(5):1697.

29. Scheller EL, Doucette CR, Learman BS, Cawthorn WA-O, Khandaker S, Schell B, et al. Region-specific variation in the properties of skeletal adipocytes reveals regulated and constitutive marrow adipose tissues. 2015.

30. Caers J, Deleu S, Belaid Z, De Raeve H, Van Valckenborgh E, De Bruyne E, et al. Neighboring adipocytes participate in the bone marrow microenvironment of multiple myeloma cells. Leukemia. 2007;21:1580.

31. Jourdan M, Tarte K, Legouffe E, Brochier J, Rossi JF, Klein B. Tumor necrosis factor is a survival and proliferation factor for human myeloma cells. European cytokine network. 1999;10(1):65-70.

32. Oranger A, Carbone C, Izzo M, Grano M. Cellular Mechanisms of Multiple Myeloma Bone Disease. Clinical and Developmental Immunology. 2013;2013:11.

33. Hajri T, Tao H, Wattacheril J, Marks-Shulman P, Abumrad NN. Regulation of adiponectin production by insulin: interactions with tumor necrosis factor-α and interleukin-6. Am J Physiol Endocrinol Metab. 2011;300(2):E350-60.

34. He Y, Lu L, Wei X, Jin D, Qian T, Yu A, et al. The multimerization and secretion of adiponectin are regulated by TNF-alpha. Endocrine. 2016;51(3):456-68.

35. Lim JY, Kim WH, Park SI. GO6976 prevents TNF-alpha-induced suppression of adiponectin expression in 3T3-L1 adipocytes: putative involvement of protein kinase C. FEBS letters. 2008;582(23-24):3473-8.

36. Chang E, Choi JM, Kim WJ, Rhee EJ, Oh KW, Lee WY, et al. Restoration of adiponectin expression via the ERK pathway in TNFalpha-treated 3T3-L1 adipocytes. Molecular medicine reports. 2014;10(2):905-10.

37. Rothenbacher D, Brenner H, Marz W, Koenig W. Adiponectin, risk of coronary heart disease and correlations with cardiovascular risk markers. European heart journal. 2005;26(16):1640-6.

38. Liu C, Feng X, Li Q, Wang Y, Li Q, Hua M. Adiponectin, TNF-alpha and inflammatory cytokines and risk of type 2 diabetes: A systematic review and meta-analysis. Cytokine. 2016;86:100-9.

39. Lihn AS, Pedersen SB, Richelsen B. Adiponectin: action, regulation and association to insulin sensitivity. Obesity reviews : an official journal of the International Association for the Study of Obesity. 2005;6(1):13-21.

40. Deng T, Lyon CJ, Bergin S, Caligiuri MA, Hsueh WA. Obesity, Inflammation, and Cancer. (1553-4014 (Electronic)).

41. Moller DE. Potential role of TNF-alpha in the pathogenesis of insulin resistance and type 2 diabetes. Trends Endocrinol Metab. 2000;11(6):212-7.

42. Hotamisligil GS, Shargill NS, Spiegelman BM. Adipose expression of tumor necrosis factor-alpha: direct role in obesity-linked insulin resistance. Science. 1993;259(5091):87-91.

43. Balkwill F. Tumour necrosis factor and cancer. Nat Rev Cancer. 2009;9(5):361-71.

44. Lemancewicz D, Bolkun L, Jablonska E, Kulczynska A, Bolkun-Skornicka U, Kloczko J, et al. Evaluation of TNF superfamily molecules in multiple myeloma patients: correlation with biological and clinical features. Leukemia research. 2013;37(9):1089-93.

Figure legends

Figure 1. **Bone marrow adiposity is increased in early stage multiple myeloma. (A)** Osmium tetroxide stained tibia analysed in a model of low tumour burden, <10% myeloma cells in bone marrow. **(B)** Total bone adiposity was measured using CT Analyser v1.13.5.1 (Bruker, Kontich, Belgium) software (24). **(C)** Immunofluorescence imaging using anti-GFP and was used to visualise the tumour area and BMAd localisation in the femur (white dotted line highlights area of tumour, red dotted line denotes tumour-bone interface). **(D)** Quantitation of BMAd number, inside and outside of the tumour area. **(E)** Paraprotein levels measured by ELISA. **(F)** Tumour burden was calculated using osteometric software. **(G)** The number of BMAds was counted using osteometric software. Data represents the mean (±SE).

Figure 2. BMAds support myeloma growth and survival. (A) ST2 cell line BMSCs and patient derived BMSCs treated with an adipogenic cocktail scale bar - 200μm. **(B)** Viability of myeloma cell lines was measured using Alamar Blue following co-culture with either media alone (NM) BMSC's or BMAds. Results are expressed as fold change relative to control cultures. Cells were cultured in normal RPMI media. Data represents the mean (±SE) of three independent experiments. Statistical significance was calculated compared to normal media (NM). **(C)** The expression of apoptotic markers was assessed by immunoblotting. **(D)** Migration was assessed using boyden chambers. Cell number in the lower chamber was measured using Alamar Blue. Data represents the mean (±SE) of four independent experiments, statistical significance was calculated compared to normal media (NM) control.

Figure 3. BMAds support myeloma cell growth by a lipid-independent mechanism. **(A)** BODIPY 493/503 staining of myeloma patient-derived lipid droplets (green) in JJN-3 cells. Scale bar 50 μm. **(B)** Lipidtox neutral red staining of ST2-derived lipid droplets in JJN-3 cells. Scale bar

50 μm. **(C)** Lipidtox neutral red staining of ST2 derived lipid droplets in 5TGM1-GFP cells. Scale bar 50 μm. All microscopy images show a representative image from four independent experiments. **(D)** The percentage of cells exhibiting lipid droplets was calculated using imageJ software. Data points represent the mean (±SE) of four independent experiments. **(E)** Viability was measured using Alamar Blue of JJN-3 and 5TGM1 cells following incubation with, normal media (NM), NM with supernatant from scraped ST2 BMSCs or NM with ST2 BMAd-derived lipid droplets. Data points represent the mean (±SE) of three independent experiments, statistical significance was calculated compared to normal media (NM) control.

Figure 4. Growth limiting conditions induce de novo lipogenesis in myeloma cells. (A) Lipidtox neutral red staining of ST2 derived lipid droplets in JJN-3 and 5TGM1 cells cultured in limiting conditions and treated with liberated lipids or conditioned media from BMAds. Scale bar 50 μm. All microscopy images show a representative image from three independent experiments. **(B)** Viability was measured using Alamar Blue. Results are expressed as fold change relative to control cultures. Cells were cultured under limiting conditions for 24 hrs followed by the addition of BMAd-derived lipid or BMAd conditioned media for a further 24 hrs. Data represents the mean (±SE) of four independent experiments, statistical significance was calculated compared to limiting media control. **(C)** Bone marrow plug taken from a 6 month old mouse 23 days post inoculation with 5TGM1 myeloma cells. Immunofluorescence of 5TGM1-GFP (green) cells and Lipidtox (red) to visualise adipocytes/lipid. Scale bars 200 μm – 50 μm respectively.

Figure 5. Myeloma cells down-regulate adiponectin in BMAds. (A) Adiponectin expression in human serum. **(B)** Bone marrow plasma concentrations of adiponectin in our experimental cohort of KaLwRij mice. **(C)** Adiponectin expression in ST2 cells co-cultured with myeloma cell lines for 24, 48, and 72 hrs was assessed by immunoblotting. **(D)** Secreted adiponectin levels in

conditioned media from ST2 cells co-cultured with myeloma cell lines for 24, 48, and 72 hrs was assessed by immunoblotting. Equal volumes of conditioned media were loaded into each lane. **(E)** *Adipoq* expression in ST2 cells co-cultured with myeloma cells for 24, 48, and 72 hrs was assessed using RT-PCR. (ND = not detectable) Data points represent the mean (±SE) of three independent experiments, statistical significance was calculated compared to ST2 alone control (no adipogenic media). **(F)** Adiponectin expression in ST2 cells co-cultured with primary human myeloma cells for 24 and 72 hrs was assessed by immunoblotting.

Figure 6. Myeloma cells reduce BMAd size and number without causing a generalised loss in adipokine secretion. (A) Oil red O stained BMAds following 72 hr direct co-culture with myeloma cells. Scale bar 50 μm. **(B)** Eluted Oil red O stain from BMAds following direct co-culture with JJN-3 or 5TGM1 cells **(C)** BMAds following 72 hr transwell co-culture with JJN-3 cells. Scale bar 50 μm. **(D)** Eluted Oil red O stain from BMAds following transwell co-culture with JJN-3 cells. **(E)** BMAds following 72 hr transwell co-culture with 5TGM1 cells. Scale bar 50 μM. **(F)** Eluted Oil red O stain from BMAds following transwell co-culture with 5TGM1 cells. Data points represent the mean (±SE) of three independent experiments, statistical significance was calculated compared to ST2 alone control. **(G)** *CFD/*Adispsin, *ADSF/*Resistin and *Nampt/*Visfatin expression was assessed by RT-PCR. Data points represent the mean (±SE) of three independent experiments, $P>0.05$, exact P values are shown in supplemental Table 1.

Figure 7. TNF-alpha down-regulates adiponectin in BMAds. (A) Correlation between bone marrow plasma-derived TNF-α and tumour burden from 5TGM1 myeloma-bearing mice. (**B**) Myeloma cells activate ERK1/2 signalling in BMAds. Protein levels of Adiponectin, P-ERK1/2, T-ERK1/2, P-JNK, T-JNK, P-P38 MAPK, T-P38 MAPK were assessed by immunoblotting in ST2-derived BMAds following 24 h treatment with 10ng/ml recombinant TNF-α or co-culture with

5TGM1 cells. **(C)** *Adipoq* expression in ST2-derived BMAds following treatment with 10 ng/ml mouse recombinant TNF-α for 24, 48 and 72 hrs was measured by RT-PCR. Percentage decrease was calculated compared to time point control. **(D)** Protein levels of adiponectin in conditioned media taken from ST2-derived BMAds following 10 ng/ml or 20 ng/ml mouse recombinant TNF-α treatment for 24, 48 or 72 hrs was assessed by immunoblotting. Equal volumes of conditioned media was loaded into each lane. **(E)** BMAds were treated with 10 ng/ml or 20 ng/ml mouse recombinant TNF-α for 72 hrs. Cells were fixed and stained with Oil red O stain. Scale bar 50 μm. Stain was eluted and absorbance measured. **(F)** BMAds were co-cultured with myeloma cells (5TGM1) in the presence or absence of an anti-TNF-α neutralising antibody. Secreted adiponectin level in the conditioned media was measured. Equal volumes of conditioned media was loaded into each lane. **(G)** Densitometry using imageJ software was used to quantify the level of secreted adiponectin shown in F. **(H)** BMAds were cultured with myeloma cells (5TGM1) in the presence or absence of an anti-TNF-α neutralising antibody and *Adipoq* expression was assessed by RT-PCR. Data points represent the mean (±SE) of three independent experiments, statistical significance was calculated compared to control. **(I)** BMAds were co-cultured with myeloma cells (5TGM1) in the presence or absence of an anti-TNF-α neutralising antibody for 72hrs. BMAds were fixed and stained with Oil red O. Stain was eluted and absorbance measured. Data points represent the mean (±SE) of six independent experiments, statistical significance was calculated compared to control.

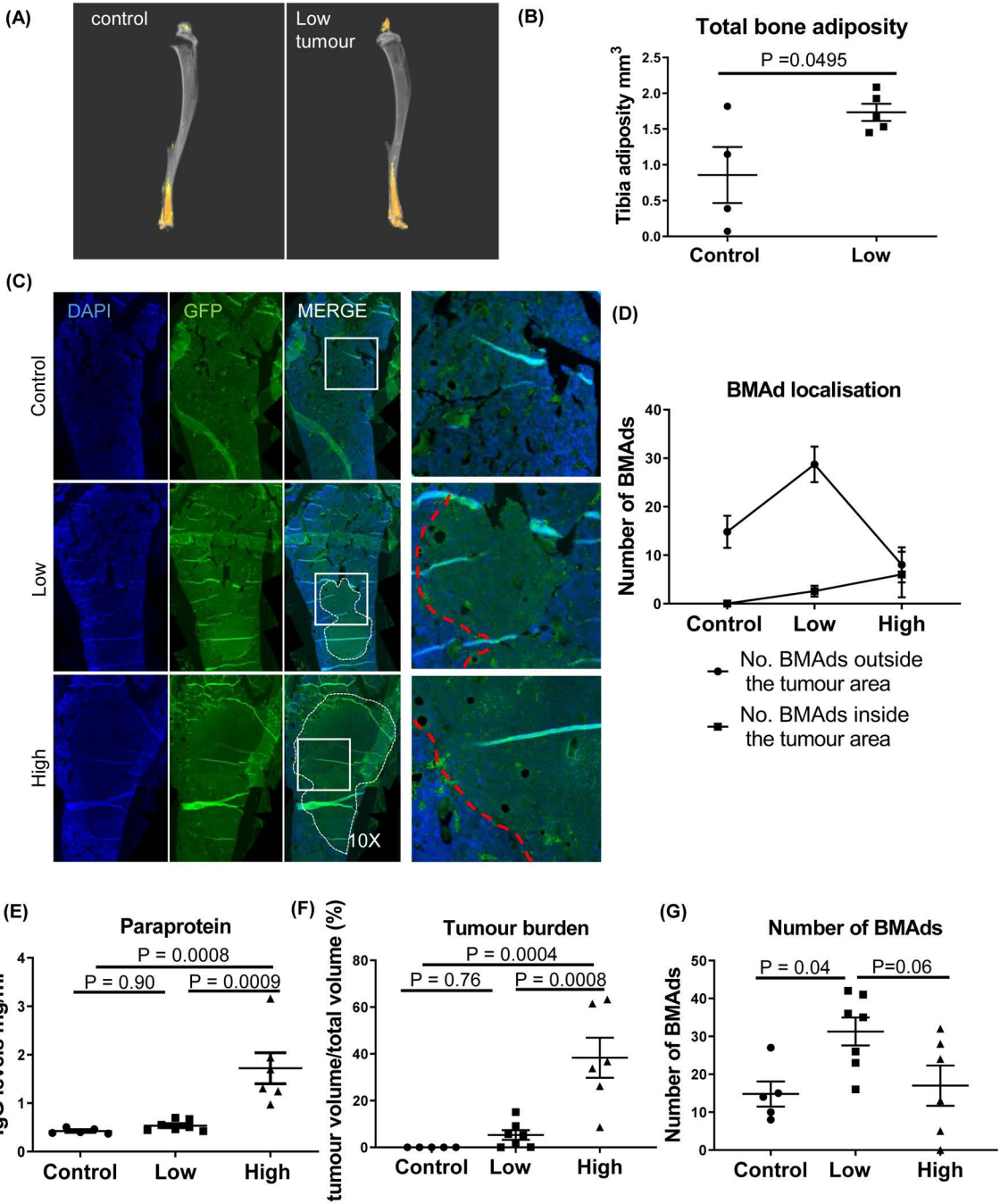
(A)
control
Low tumour
(B)
Total bone adiposity
P =0.0495
Tibia adiposity mm3
2.5
2.0
1.5
1.0
0.5
0.0
Control
Low
(C)
DAPI
GFP
MERGE
Control
Low
High
10X
(D)
BMAd localisation
Number of BMAds
40
30
20
10
0
Control
Low
High
No. BMAds outside the tumour area
No. BMAds inside the tumour area
(E)
Paraprotein
P = 0.0008
P = 0.90
P = 0.0009
IgG levels mg/ml
4
3
2
1
0
Control
Low
High
(F)
Tumour burden
P = 0.0004
P = 0.76
P = 0.0008
tumour volume/total volume (%)
80
60
40
20
0
Control
Low
High
(G)
Number of BMAds
P = 0.04
P=0.06
Number of BMAds
50
40
30
20
10
0
Control
Low
High

Figure 1

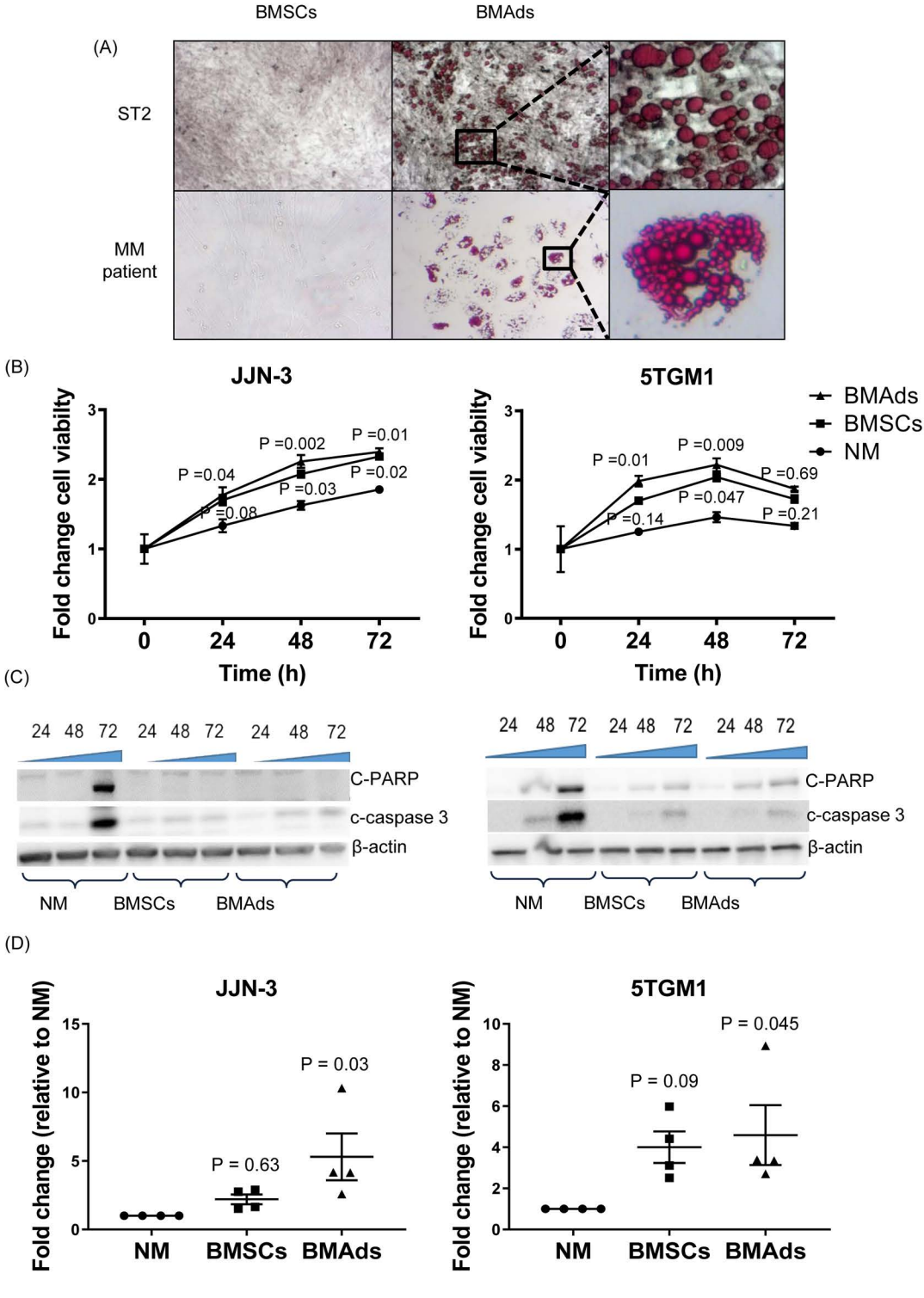
BMSCs
BMAds
(A)
ST2
MM patient
(B)
JJN-3
5TGM1
Fold change cell viabilty
Time (h)
BMAds
BMSCs
NM
P =0.04
P =0.08
P =0.002
P =0.03
P =0.01
P =0.02
P =0.01
P =0.14
P =0.009
P =0.047
P =0.69
P =0.21
(C)
24 48 72
C-PARP
c-caspase 3
β-actin
NM
BMSCs
BMAds
(D)
JJN-3
5TGM1
Fold change (relative to NM)
P = 0.63
P = 0.03
P = 0.09
P = 0.045

Figure 2

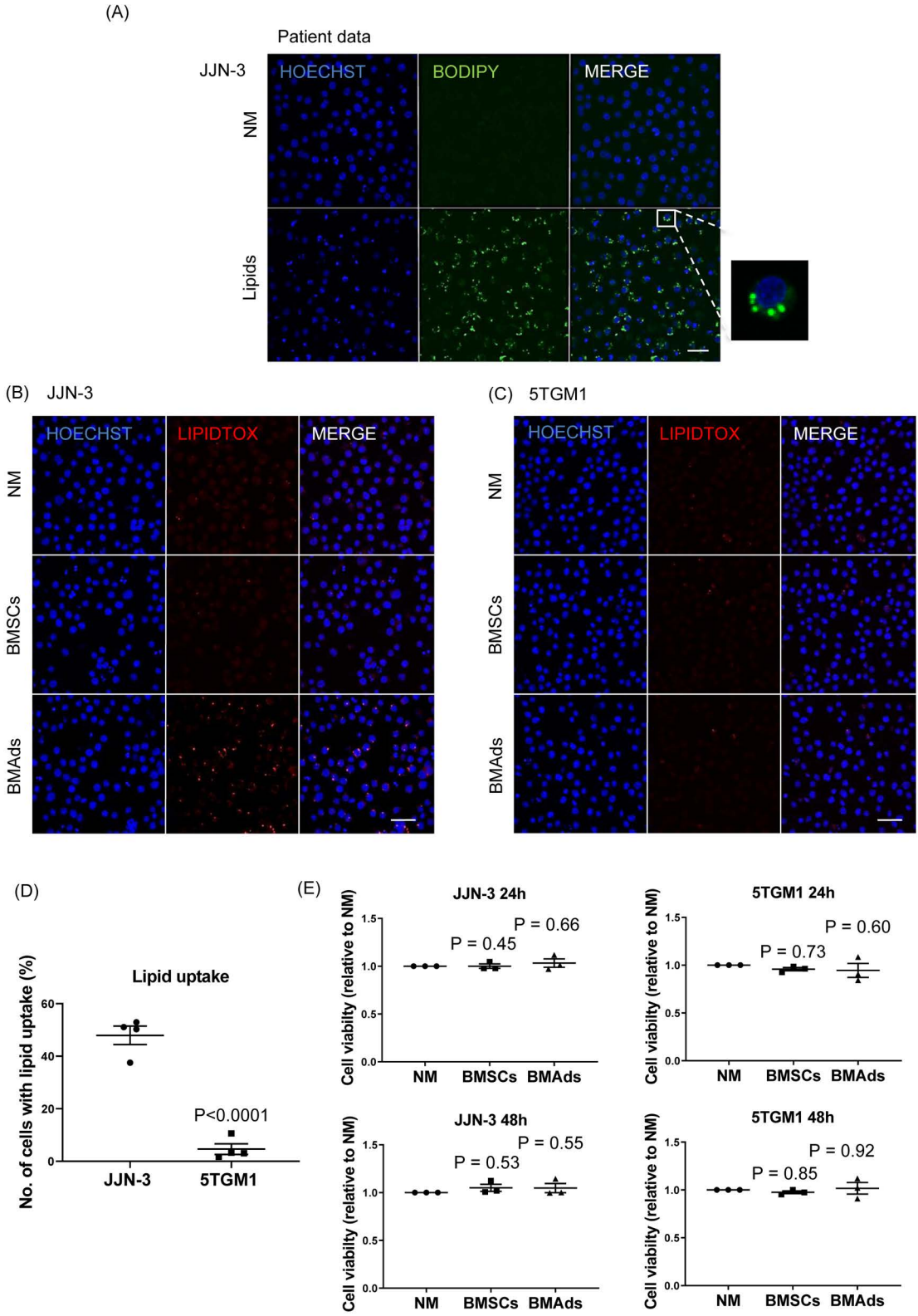
(A)
Patient data
JJN-3
HOECHST
BODIPY
MERGE
NM
Lipids
(B) JJN-3
HOECHST
LIPIDTOX
MERGE
NM
BMSCs
BMAds
(C) 5TGM1
HOECHST
LIPIDTOX
MERGE
NM
BMSCs
BMAds
(D)
Lipid uptake
No. of cells with lipid uptake (%)
60
40
20
0
P<0.0001
JJN-3
5TGM1
(E)
JJN-3 24h
P = 0.66
P = 0.45
5TGM1 24h
P = 0.60
P = 0.73
JJN-3 48h
P = 0.55
P = 0.53
5TGM1 48h
P = 0.92
P = 0.85
Cell viability (relative to NM)
1.5
1.0
0.5
0.0
NM
BMSCs
BMAds

Figure 3

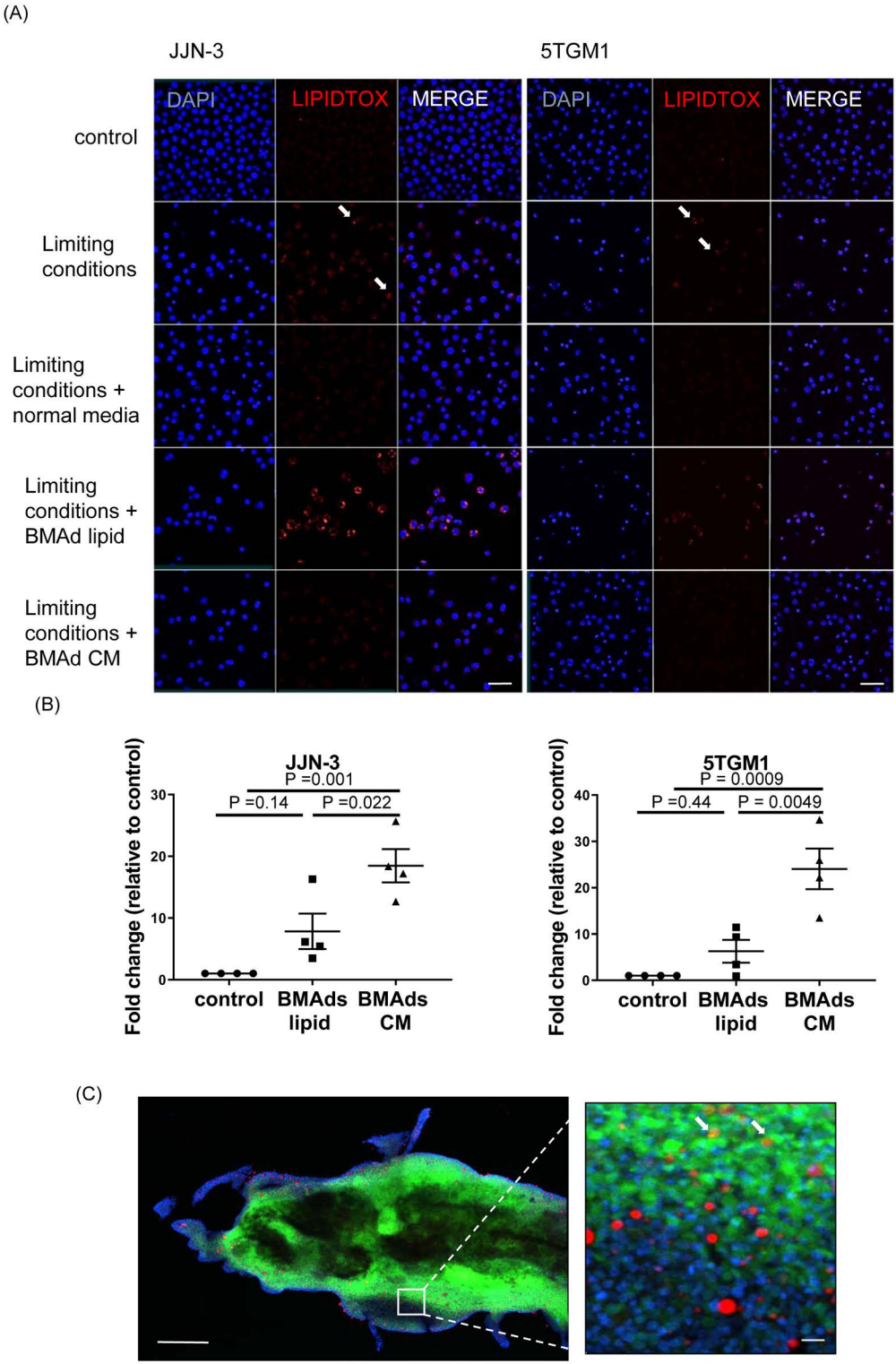
(A)
JJN-3
5TGM1
DAPI
LIPIDTOX
MERGE
control
Limiting conditions
Limiting conditions + normal media
Limiting conditions + BMAd lipid
Limiting conditions + BMAd CM
(B)
JJN-3
P =0.001
P =0.14
P =0.022
Fold change (relative to control)
control
BMAds lipid
BMAds CM
5TGM1
P = 0.0009
P =0.44
P = 0.0049
(C)

Figure 4

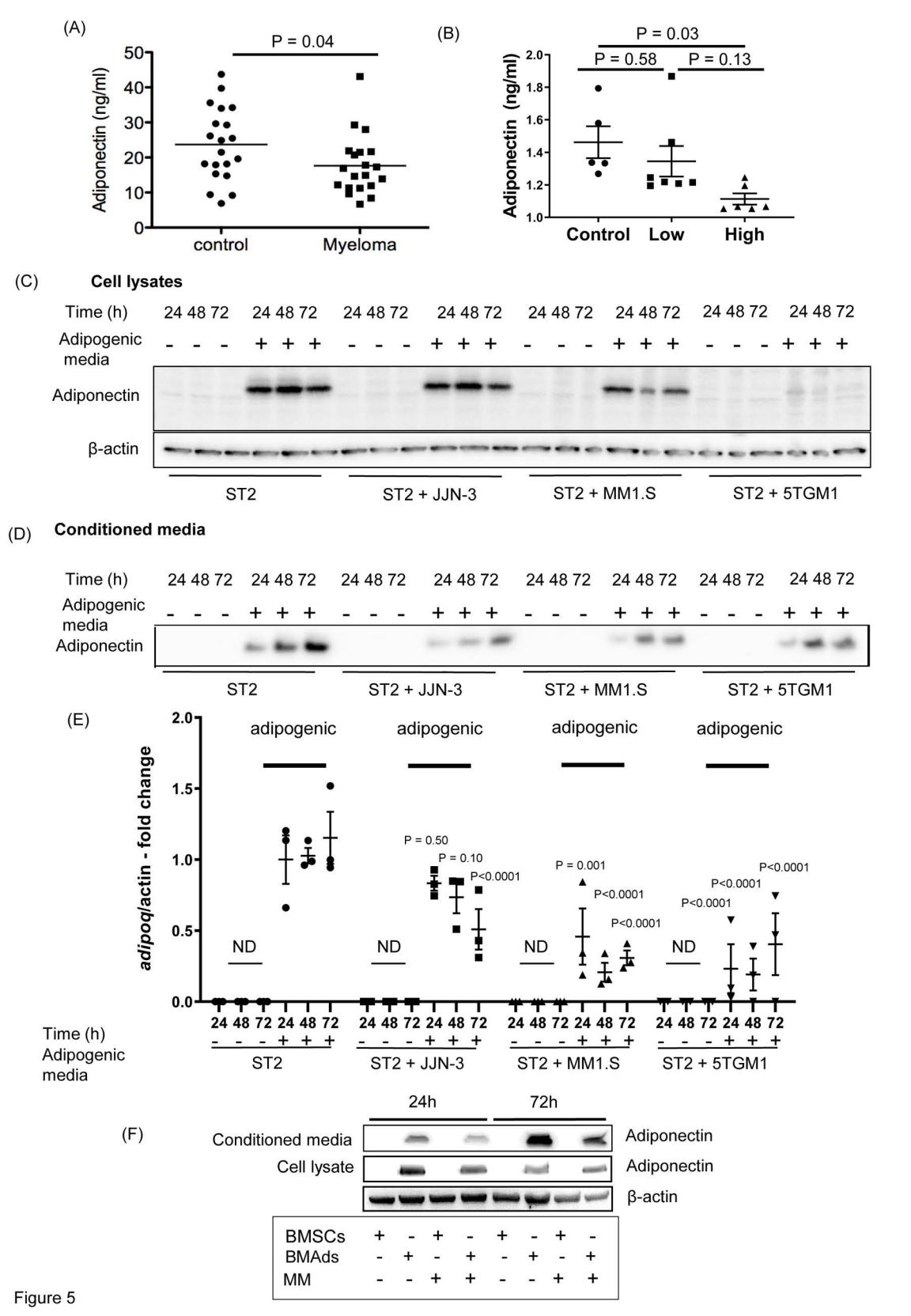
(A)
P = 0.04
Adiponectin (ng/ml)
50
40
30
20
10
0
control
Myeloma
(B)
P = 0.03
P = 0.58
P = 0.13
Adiponectin (ng/ml)
2.0
1.8
1.6
1.4
1.2
1.0
Control
Low
High
(C)
Cell lysates
Time (h)
24 48 72 24 48 72 24 48 72 24 48 72 24 48 72 24 48 72 24 48 72 24 48 72
Adipogenic media
- - - + + + - - - + + + - - - + + + - - - + + +
Adiponectin
β-actin
ST2
ST2 + JJN-3
ST2 + MM1.S
ST2 + 5TGM1
(D)
Conditioned media
Time (h)
24 48 72 24 48 72 24 48 72 24 48 72 24 48 72 24 48 72 24 48 72 24 48 72
Adipogenic media
- - - + + + - - - + + + - - - + + + - - - + + +
Adiponectin
ST2
ST2 + JJN-3
ST2 + MM1.S
ST2 + 5TGM1
(E)
adipoq/actin - fold change
2.0
1.5
1.0
0.5
0.0
adipogenic
adipogenic
adipogenic
adipogenic
ND
ND
ND
ND
P = 0.50
P = 0.10
P<0.0001
P = 0.001
P<0.0001
P<0.0001
P<0.0001
P<0.0001
P<0.0001
Time (h)
Adipogenic media
24 48 72 24 48 72 24 48 72 24 48 72
- - - + + + - - - + + + - - - + + + - - - + + +
ST2
ST2 + JJN-3
ST2 + MM1.S
ST2 + 5TGM1
(F)
24h
72h
Conditioned media
Cell lysate
Adiponectin
Adiponectin
β-actin
BMSCs + - + - + - + -
BMAds - + - + - + - +
MM - - + + - - + +

Figure 5

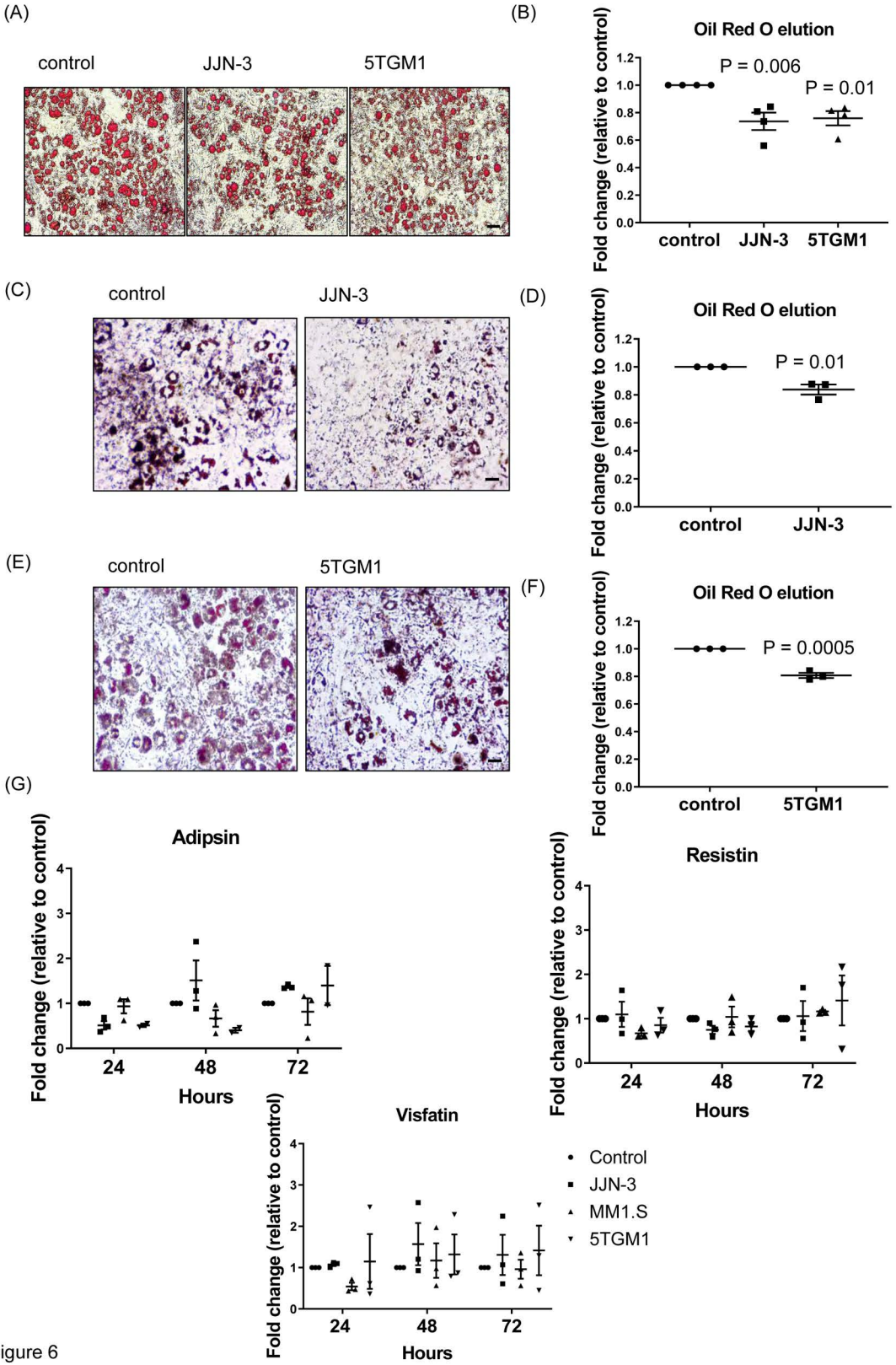
(A)
control
JJN-3
5TGM1
(B)
Oil Red O elution
P = 0.006
P = 0.01
Fold change (relative to control)
control
JJN-3
5TGM1
(C)
control
JJN-3
(D)
Oil Red O elution
P = 0.01
Fold change (relative to control)
control
JJN-3
(E)
control
5TGM1
(F)
Oil Red O elution
P = 0.0005
Fold change (relative to control)
control
5TGM1
(G)
Adipsin
Fold change (relative to control)
Hours
24
48
72
Resistin
Visfatin
Control
JJN-3
MM1.S
5TGM1

Figure 6

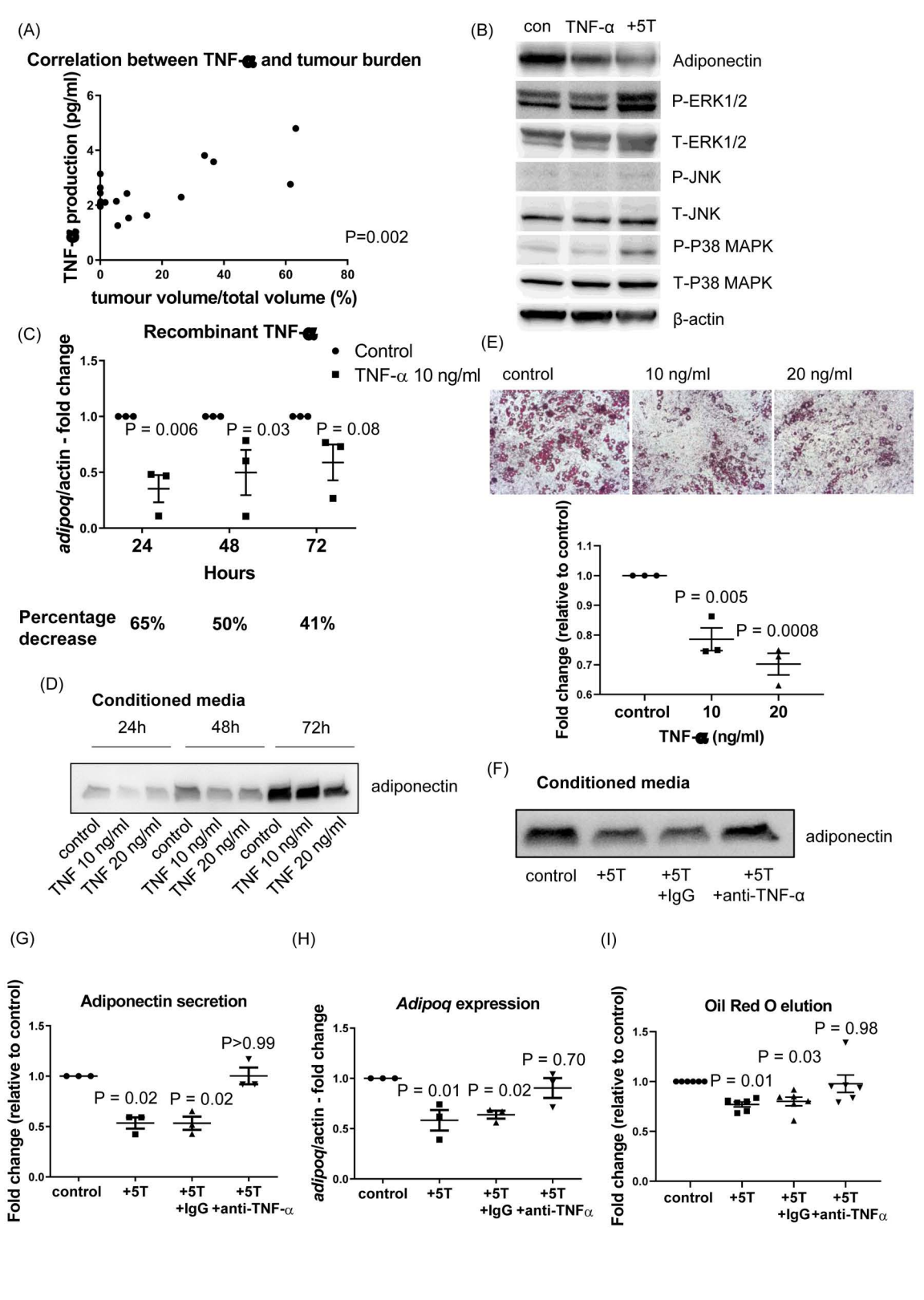
(A)
Correlation between TNF-α and tumour burden
TNF-α production (pg/ml)
tumour volume/total volume (%)
P=0.002
(B)
con
TNF-α
+5T
Adiponectin
P-ERK1/2
T-ERK1/2
P-JNK
T-JNK
P-P38 MAPK
T-P38 MAPK
β-actin
(C)
Recombinant TNF-α
Control
TNF-α 10 ng/ml
adipoq/actin - fold change
P = 0.006
P = 0.03
P = 0.08
Hours
Percentage decrease
65%
50%
41%
(D)
Conditioned media
24h
48h
72h
adiponectin
control
TNF 10 ng/ml
TNF 20 ng/ml
(E)
control
10 ng/ml
20 ng/ml
Fold change (relative to control)
P = 0.005
P = 0.0008
TNF-α (ng/ml)
(F)
Conditioned media
adiponectin
control
+5T
+5T +IgG
+5T +anti-TNF-α
(G)
Adiponectin secretion
Fold change (relative to control)
P = 0.02
P = 0.02
P>0.99
control
+5T
+5T +IgG
+5T +anti-TNF-α
(H)
Adipoq expression
adipoq/actin - fold change
P = 0.01
P = 0.02
P = 0.70
control
+5T
+5T +IgG
+5T +anti-TNFα
(I)
Oil Red O elution
Fold change (relative to control)
P = 0.01
P = 0.03
P = 0.98
control
+5T
+5T +IgG
+5T +anti-TNFα

Figure 7

Supplemental Data

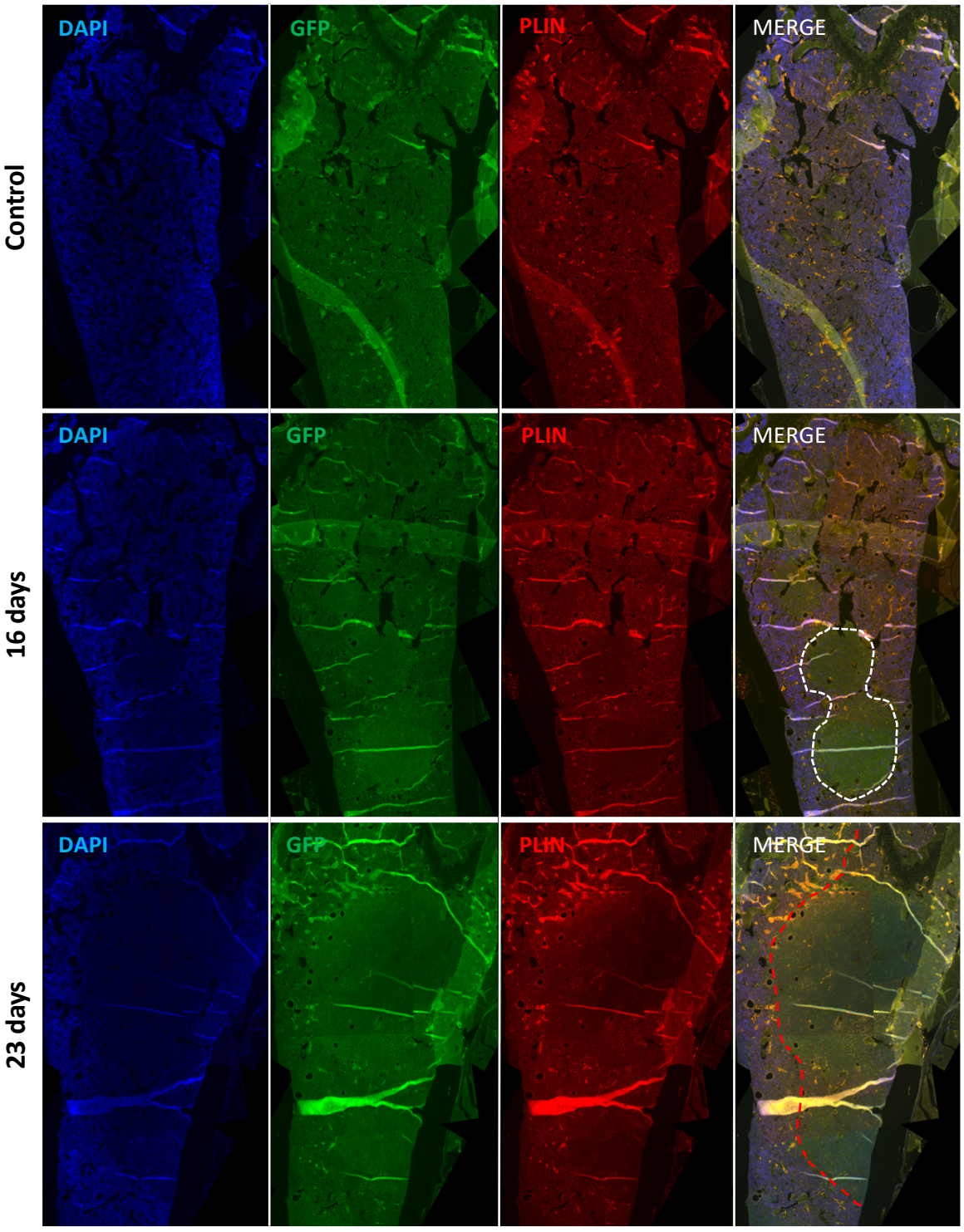

Supplemental Figure 1. BMAds predominantly locate along the tumour-bone interface. Formalin fixed sections stained with anti-GFP and Perilipin to visualise BMAd location in the femur (white circle highlights tumour area, red dotted line denotes bone-tumour interface).

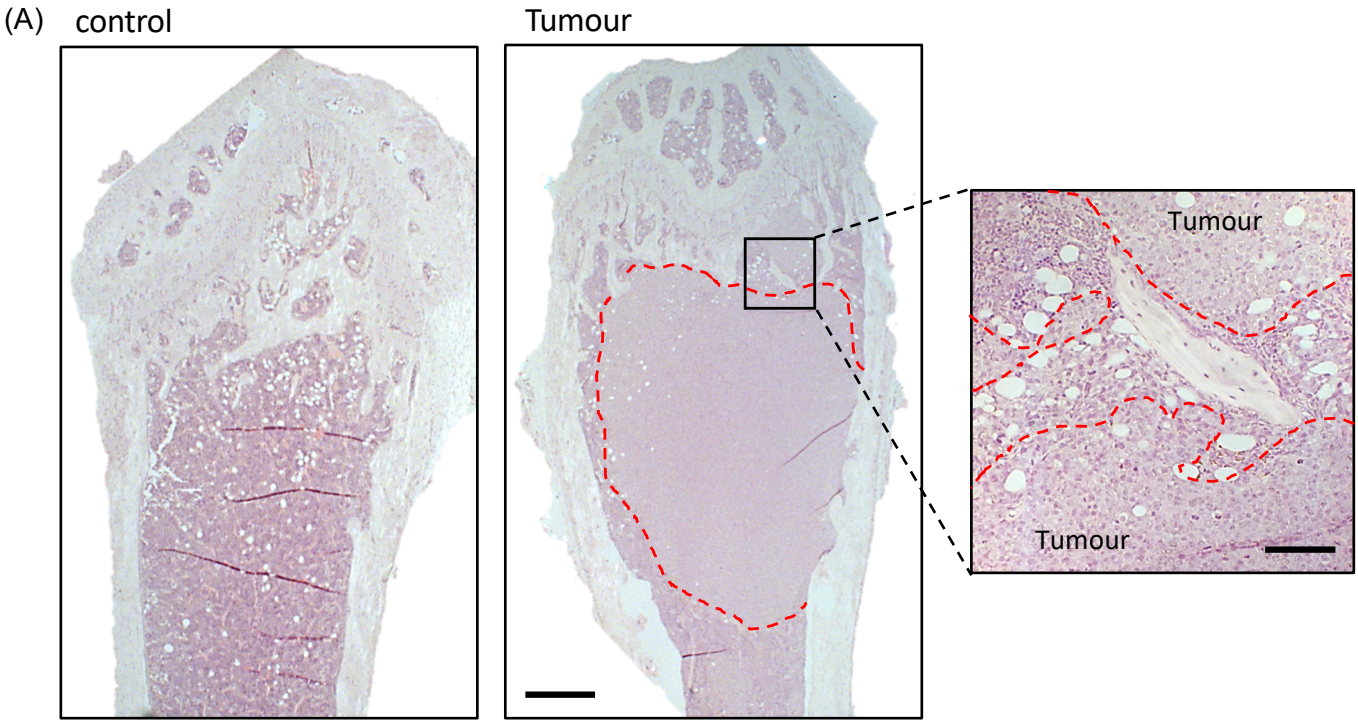

Supplemental Figure 2. Adipocytes localise to the tumour-bone interface in a human model of multiple myeloma. NOD/SCID/gamma mice were injected with JJN-3 myeloma cells and developed aggressive short-term disease. Tumour areas were identified as light patches of cells within the marrow. Tumour-bone interface is denoted by red dotted line. Scale bar 500 µm. Additional box shows a higher magnification to show the BMAds surrounding the tumour area (red dotted line denotes tumour-bone interface). Scale bar 100 µm.

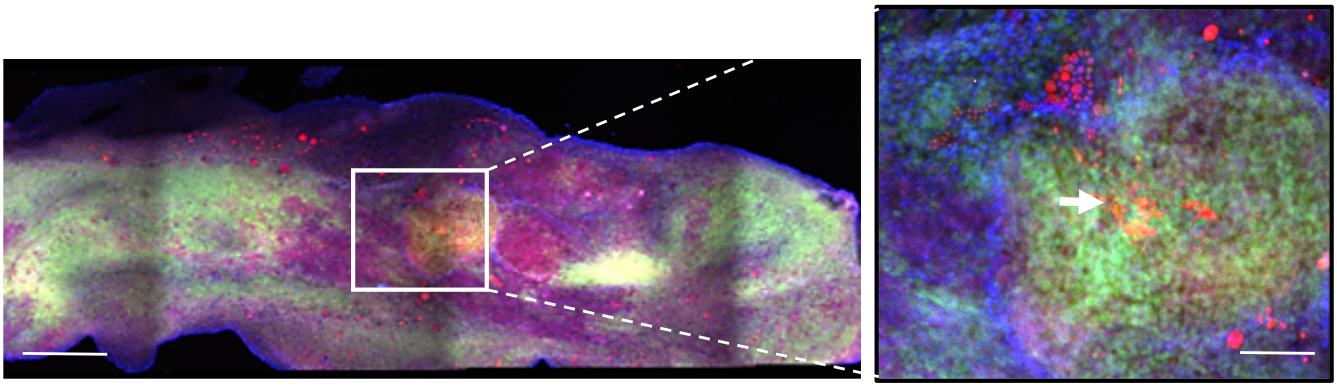

Supplemental Figure 3. 5TGM1-GFP cells uptake lipid *in vivo*. Immunofluorescence of 5TGM1-GFP (green) cells and Lipidtox (red) to visualise adipocytes/lipid. Scale bars 200 μm – 50 μm.

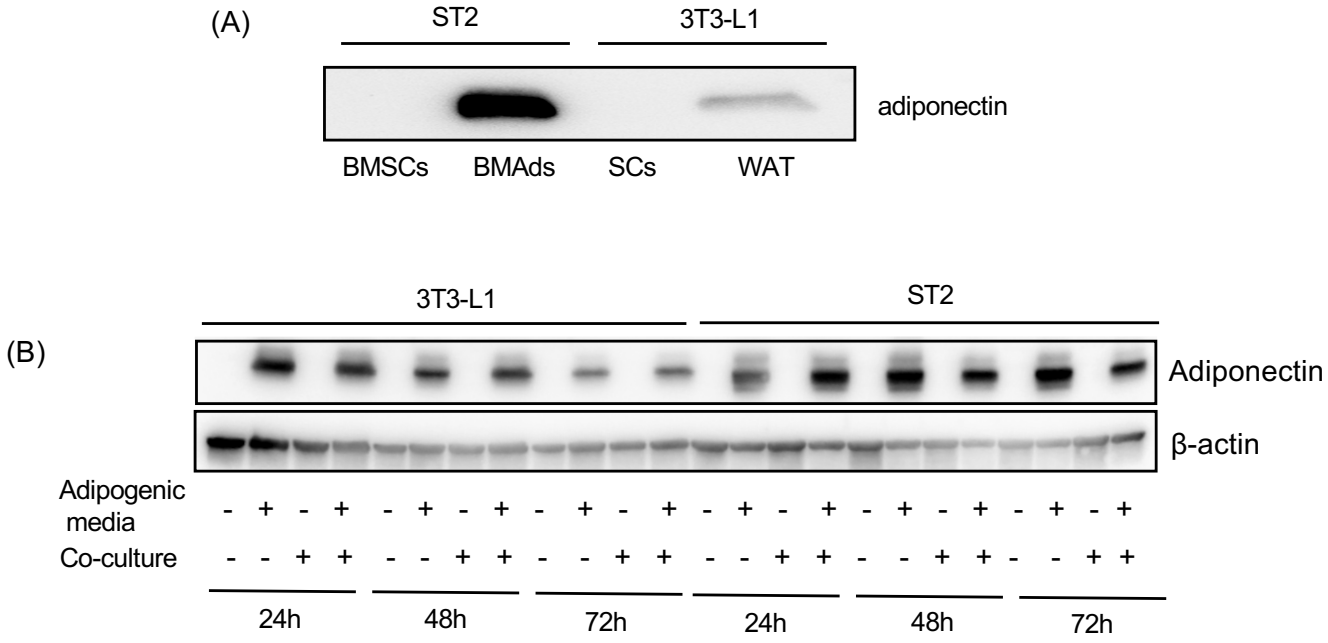

Figure 4. Myeloma cells decrease adiponectin expression in BMAds but not in WAT-like adipocytes (A) Adiponectin protein expression was measured in conditioned media taken from undifferentiated (BMSCs/SCs) and differentiated (BMAds/WAT) ST2 cells and 3T3-L1 cells using immunoblotting. **(B)** Adiponectin expression in BMSCs/SCs and BMAds/WAT cultured alone or in co-culture with 5TGM1 myeloma cells.

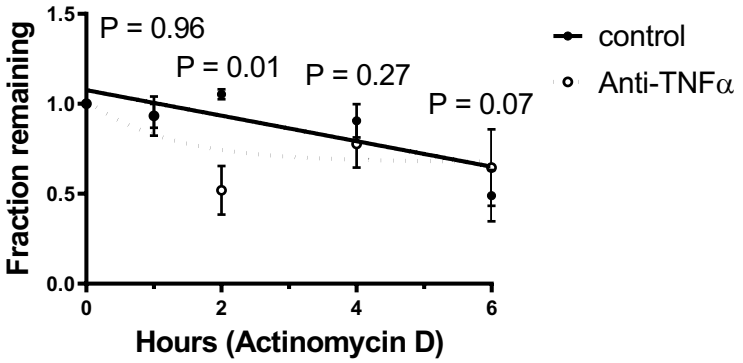

Supplemental Figure 5. TNF-α treatment causes *Adipoq* mRNA instability in ST2-derived BMAds. BMAds were treated for 24 hrs with 10ng/ml of TNF-α, *Adipoq* mRNA stability was assessed by qPCR following the addition of 10μg/ml actinomycin D for 0, 1, 2, 4 or 6 hours. Data points represent the mean (±SE) of three independent experiments. Statistical analysis is compared to 0 hrs control.

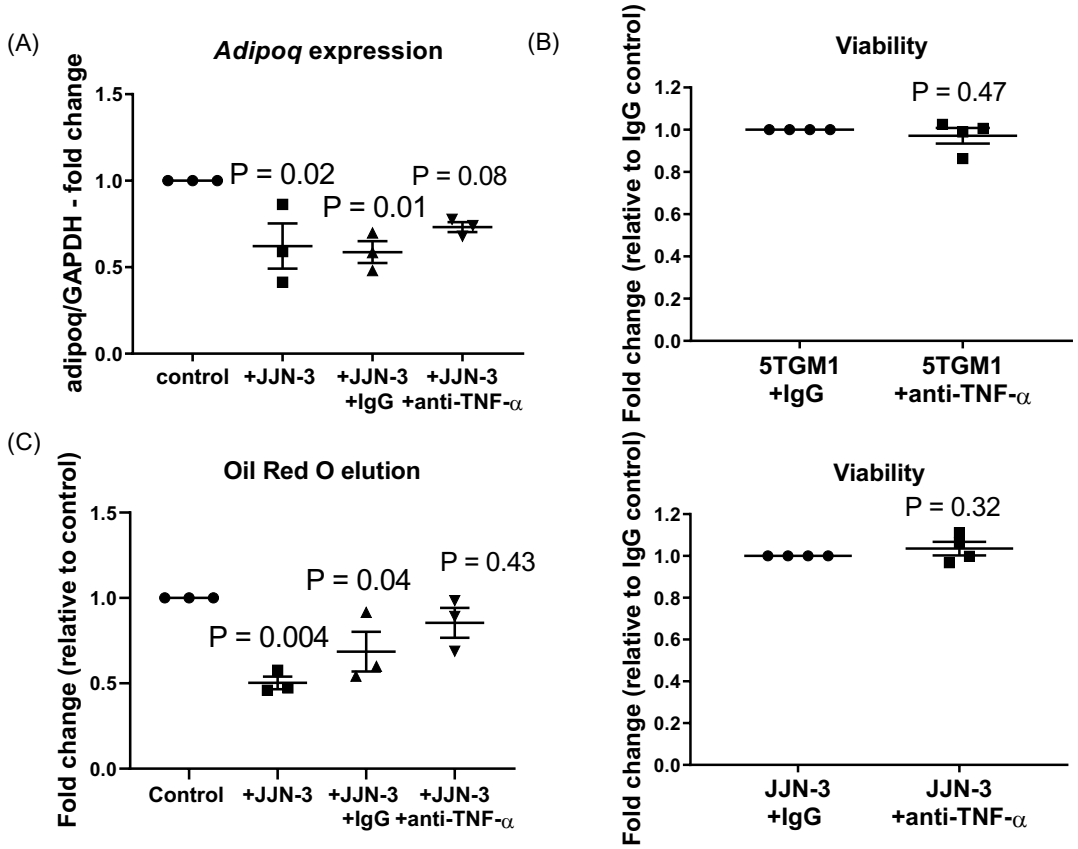

Supplemental Figure 6. TNF-α treatment decreases *Adipoq* expression. (A) BMAds were cultured with myeloma cells (JJN-3) for 48 h in the presence or absence of an anti-TNF-α neutralising antibody, *Adipoq* expression was assessed by RT-PCR. Data points represent the mean (±SE) of three independent experiments. Statistical analysis is compared to control. **(B)** Viability was measured using Alamar Blue. Results are expressed as fold change relative to IgG control. Data points represent the mean (±SE) of four independent experiments. **(C)** BMAds were cultured with myeloma cells (JJN-3) for 72 hrs in the presence or absence of an anti-TNF-α neutralising antibody, cells were fixed and stained with Oil red O. The stain was eluted and the absorbance measured. Data points represent the mean (±SE) of three independent experiments. Statistical analysis is compared to control.

Hours	Dunnett's multiple comparisons test	Adipsin (adjusted P value)	Resistin (adjusted P value)	Visfatin (adjusted P value)
24	Control vs. JJN-3	0.2303	0.9801	0.9981
24	Control vs. MM1.S	0.9913	0.6181	0.7367
24	Control vs. 5TGM1	0.3120	0.9402	0.9856
48	Control vs. JJN-3	0.2011	0.7767	0.5995
48	Control vs. MM1.S	0.5149	0.9986	0.9787
48	Control vs. 5TGM1	0.1744	0.9060	0.8862
72	Control vs. JJN-3	0.4351	0.9956	0.8950
72	Control vs. MM1.S	0.8552	0.9197	0.9997
72	Control vs. 5TGM1	0.4670	0.4469	0.7853

Supplemental Table 1. P values associated with Figure 6G. *CFD*/Adispsin, *ADSF*/Resistin and *Nampt*/Visfatin expression was assessed by RT-PCR. Data points represent the mean (±SE) of three independent experiments. Data was analysed using a 2 way ANOVA. statistical significance was calculated compared to control.